Eur. Phys. J. Appl. Phys. **33**, 97–101 (2006)
DOI: 10.1051/epjap:2006009

**THE EUROPEAN PHYSICAL JOURNAL APPLIED PHYSICS**

# Voltage sources in a $-\chi$ discrete geometric approach to eddy-currents

R. Specogna[a] and F. Trevisan

Dip. di Ingegneria Elettrica, Gestionale e Meccanica, Università di Udine, Via delle Scienze 208, 33100 Udine, Italy

Received: 17 February 2005 / Received in final form: 23 June 2005 / Accepted: 25 October 2005
Published online: 8 February 2006 – 

**Abstract.** We propose a pair of approaches to account for voltage driven coils when solving 3D eddy-current problems with a *discrete geometric* approach. The formulation we use is based on the circulation $a$ of the magnetic vector potential on primal edges and on a scalar potential $\chi$ on conductor primal nodes. The proposed approaches consider distributed or localized voltage sources respectively and they can be applied to general coil geometries. The results are compared with those obtained with Finite Elements.

**PACS.** 02.70.-c Computational techniques – 41.20.Gz Magnetostatics; magnetic shielding, magnetic induction, boundary-value problems

## 1 Introduction

The modeling of voltage driven coils as sources in eddy-current problems is a well known problem and efficient solutions have been proposed in [1,2,7] in the framework of Finite Elements formulations. We will start here from an algebraic formulation for eddy-currents [10] deduced from the so called *discrete geometric* approach [15]. This formulation, named $a-\chi$, is based on the circulation of magnetic vector potential $a$ on primal edges and on a scalar potential $\chi$ on primal nodes of a mesh made of a pair of interlocked cell complexes. The aim of this paper is to introduce the algebraic equations of voltage driven coils within the $a-\chi$ formulation, which "naturally" treats only current driven coils.

In order to specify the sources in terms of imposed e.m.f.s along a set of primal edges, we will propose two strategies. In the first strategy e.m.f.s are determined on all the primal edges of the source region (Distributed Voltage Sources), while, in the second one, only a subset of edges of the source region have the e.m.f.s assigned (Localized Voltage Source). We will also propose an iterative algorithm to make consistent the right-hand side term of the final linear system, in the case of Distributed Voltage Sources; in this way the construction of the right-hand side of the final system is simplified. The performances of the two strategies will be compared with respect to a numerical example.

## 2 a $-\chi$ formulation for voltage driven coils

The domain of interest $D$ of the eddy-current problem, can be partitioned into a source region $D_s$, consisting of a voltage driven coil, a passive conductive region $D_c$, and an air region $D_a$ which is the complement of $D_c$ and $D_s$ in $D$. We introduce in $D$ a pair of interlocked cell complexes [3,6,14]. The primal complex is simplicial with *inner* oriented cells such as nodes $n$, edges $e$, faces $f$, volumes $v$ ($v$ are tetrahedra).

The dual complex is obtained from the primal according to the barycentric subdivision, with *outer* oriented cells such as dual volumes $\tilde{n}$, dual faces $\tilde{e}$, dual edges $\tilde{f}$, dual nodes $\tilde{v}$. For example a dual node $\tilde{v}$ is the barycenter of the tetrahedron $v$, a dual edge $\tilde{f}$ is line drawn from the barycenter of $f$ joining the two dual nodes $\tilde{v}'$, $\tilde{v}''$ in the tetrahedra $v'$, $v''$ on both sides of $f$; with this notation the one-to-one correspondence between a cell and its dual becomes evident.

The interconnections between cells of the primal complex, are defined by the usual connectivity matrices $\mathbf{G}$ between pairs $(e,n)$, $\mathbf{C}$ between pairs $(f,e)$, $\mathbf{D}$ between pairs $(v,f)$. Similarly, the corresponding matrices for the dual complex are $-\mathbf{G}^T$ (the minus sign is due to the assumption that a dual volume $\tilde{n}$ is oriented by the outward normal, while a node $n$ is oriented as a sink) between pairs $(\tilde{n},\tilde{e})$, $\mathbf{C}^T$ between pairs $(\tilde{e},\tilde{f})$ and $\mathbf{D}^T$ between pairs $(\tilde{f},\tilde{v})$. With respect to these cell complexes[1], we recall the physical laws governing an eddy-current problem, written at discrete level, without any approximation, in terms of

[a] e-mail: r.specogna@nettuno.it

[1] In a cell complex, properties $\mathbf{CG}=0$ and $\mathbf{DC}=0$ hold.

the Degrees of Freedom arrays

$$\begin{aligned} \mathbf{D}\,\mathbf{b} &= \mathbf{0} && \text{(a)} \\ \mathbf{C}\,\mathbf{e} &= -d_t\mathbf{b} && \text{(b)} \\ \mathbf{C}^T\,\mathbf{h} &= \mathbf{j} && \text{(c)} \\ \mathbf{G}^T\,\mathbf{j} &= \mathbf{0} && \text{(d)} \end{aligned} \qquad (1)$$

where (a) is Gauss's law relating the array $\mathbf{b}$ of magnetic induction fluxes associated with primal faces (the $k$-th entry of $\mathbf{b}$ is in Wb), (b) is Faraday's law relating the array $\mathbf{e}$ of e.m.f.s along primal edges (the $k$-th entry of $\mathbf{e}$ is in V), (c) is Ampère's law relating the array $\mathbf{h}$ of m.m.f.s associated with dual edges (the $k$-th entry of $\mathbf{h}$ is in A) and $\mathbf{j}$ is the array of currents crossing dual faces (the $k$-th entry of $\mathbf{j}$ is in A), (d) is the *continuity* law. We wrote (1a) and (1d) explicitly even though the are implied by (1b) and (1c) respectively, because we use them to deduce the final system of equations.

In addition to these laws, discrete counterparts of constitutive laws have to be considered

$$\mathbf{h} = \boldsymbol{\nu}\,\mathbf{b}, \qquad \mathbf{j} = \boldsymbol{\sigma}\,(\mathbf{e} + \mathbf{e}^s), \qquad (2)$$

where $\boldsymbol{\nu}$ ($\dim(\boldsymbol{\nu}) = N_f$, $N_f$ being the number of faces in $D$) and $\boldsymbol{\sigma}$ (its dimension depends on the number of edges in the conducting region considered) are some square mesh- and medium-dependent matrices that require *metric* notions and *material* properties in order to be computed [13]. We indicate with $\boldsymbol{\sigma}_c$ Ohm's matrix in $D_c$ with $\dim(\boldsymbol{\sigma}_c) = N_{ec}$ and with $\boldsymbol{\sigma}_s$ Ohm's matrix in $D_s$ with $\dim(\boldsymbol{\sigma}_s) = N_{es}$, where $N_{ec}$ and $N_{es}$ are the numbers of edges in $D_c$ and $D_s$ respectively.

The magnetic matrix $\boldsymbol{\nu}$ can be computed as described in [11], while Ohm's matrix $\boldsymbol{\sigma}$ can be computed as proposed in [10,12]; it may be non-symmetric and may differ from the one used in finite elements [1]. Alternative approaches are suggested in [4,5]. Finally, we have indicated with $\mathbf{e}^s$ the array of imposed e.m.f.s along primal edges of $D_s$.

We recall briefly the $a-\chi$ formulation [10]. We search for $\mathbf{u}$ as a sum of arrays $\mathbf{a} + \mathbf{G}\,\boldsymbol{\chi}$, where $\mathbf{a}$ is the array of circulations $a$ of the magnetic vector potential along primal edges $e$ of $D$ and $\boldsymbol{\chi}$ is the array of scalar potential $\chi$ associated with primal nodes $n$ of $D_c$ and $D_s$. In this way (1a) is satisfied identically and we may rewrite (1) with (2) using $\mathbf{u}$, obtaining the following equations in the frequency domain ($d_t \to i\omega$),

$$\begin{aligned} &(\mathbf{C}^T\boldsymbol{\nu}\mathbf{C}\mathbf{a})_e = 0 && \forall\, e \in D_a \\ &(\mathbf{C}^T\boldsymbol{\nu}\mathbf{C}\mathbf{a})_e + i\omega(\boldsymbol{\sigma}_s\mathbf{a}_s)_e + i\omega(\boldsymbol{\sigma}_s\mathbf{G}_s\boldsymbol{\chi}_s)_e = (\mathbf{j}^s)_e && \forall\, e \in D_s \\ &(\mathbf{C}^T\boldsymbol{\nu}\mathbf{C}\mathbf{a})_e + i\omega(\boldsymbol{\sigma}_c\mathbf{a}_c)_e + i\omega(\boldsymbol{\sigma}_c\mathbf{G}_c\boldsymbol{\chi}_c)_e = 0 && \forall\, e \in D_c \\ &i\omega(\mathbf{G}_s^T\boldsymbol{\sigma}_s\mathbf{a}_s)_n + i\omega(\mathbf{G}_s^T\boldsymbol{\sigma}_s\mathbf{G}_s\boldsymbol{\chi}_s)_n = (\mathbf{G}_s^T\mathbf{j}^s)_n && \forall\, n \in D_s \\ &i\omega(\mathbf{G}_c^T\boldsymbol{\sigma}_c\mathbf{a}_c)_n + i\omega(\mathbf{G}_c^T\boldsymbol{\sigma}_c\mathbf{G}_c\boldsymbol{\chi}_c)_n = 0 && \forall\, n \in D_c, \end{aligned} \qquad (3)$$

where arrays $\mathbf{a}_r$ or $\boldsymbol{\chi}_r$, with $r = \{s, c\}$, are the sub-arrays of $\mathbf{a}$ or $\boldsymbol{\chi}$ respectively, associated with primal edges or nodes in $D_r$; similarly $\mathbf{G}_r$ is the sub-matrix of $\mathbf{G}$ associated with pairs $(e, n)$ of $D_r$. With $(\mathbf{x})_k$ we mean the $k$-th row of array $\mathbf{x}$, where $k = \{e, n\}$ is the label of edge $e$ or of node $n$. In the right-hand side of (3), we introduced the array $\mathbf{j}^s$ of *equivalent source* currents defined as

$$\mathbf{j}^s = \boldsymbol{\sigma}_s\mathbf{e}^s, \qquad (4)$$

indexed over the edges of $D_s$. The system (3) is singular and to solve it we rely on CG method without gauge condition [8].

In the following we will describe the strategies of Distributed Voltage Source and of Localized Voltage Source respectively to construct the right-hand side of the system (3). In both the proposed approaches, array $\mathbf{j}^s$ will be not consistent with (1d). However, we will show how to guarantee consistency of the right-hand side at least for one of the two approaches (the Distributed Voltage Source case). When consistency holds, the last two sets of equations in (3) are implied by the first three sets, yielding no new information and thus they can be omitted; also $\chi$ can be omitted and we obtain the so called $a$-formulation [9]. To solve (3) we adopt a CG iterative solver (with SSOR preconditioner) and to achieve a good convergence rate in the case of $a$-formulation, special preconditioners must be exploited, see [16,17]; for this reason we will use here the $a-\chi$ formulation also when consistency holds.

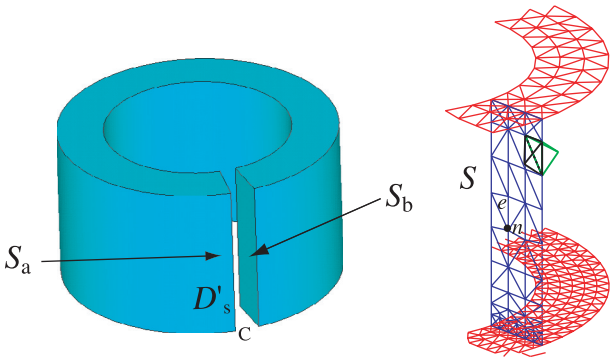


**Fig. 1.** On the left the coil with the air cut are shown, together with the pair of surfaces $S_a$, $S_b$ between the thick cut $C$ and the conductor. On the right nodes like $n$ and edges like $e$ laying on $S$ have duplicated labels.

## 3 Distributed voltage sources

In the case of particular symmetries of $D_s$, the imposed electric field $\mathrm{E}^s(P)$ at a point $P \in D_s$ can be computed in advance. In this case we derive immediately the e.m.f. $e^s_e = \int_e \mathrm{E}^s \cdot dl$ along edge $e$ and thus construction of the right-hand side of (3) is straightforward.

In the case of a generic coil geometry, we consider a thick cut in $D_s$ by introducing an insulating volume $C$. Then to compute $\mathrm{E}^s$, we solve a steady-state conduction current problem in the sub-domain $D'_s = D_s - C$ with assigned boundary conditions on the two surfaces $S_a$, $S_b$ between $C$ and $D'_s$, Figure 1. Thinking to a limit process, we can make the thick cut $C$ thinner and thinner until $S_a$ and $S_b$ coincide with the two faces of a single cut surface $S$ (Fig. 1, on the right). Thence, labels of nodes and edges

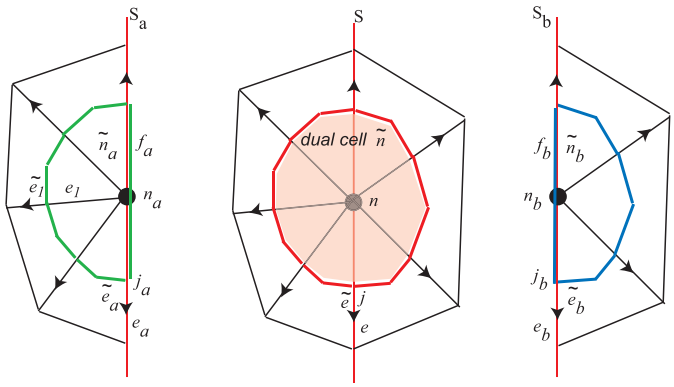


**Fig. 2.** Schematic 2D view of a dual cell $\tilde{n}$. A node $n$ on $S$ is identified by two distinct labels $n_a$, $n_b$ indicating topologically two different nodes but with the same coordinates, similarly for edges like $e$ on $S$.

laying on the cut surface $S$ are duplicated (in Fig. 1, on the right, nodes like $n$ and edges like $e$). To account for this, we have to write a new incidence matrix $\mathbf{G}'_s$ between edges and nodes within domain $D'_s$ only.

Now, we deduce the algebraic equations governing a discrete steady-state conduction current problem in $D'_s$. We substitute in (1d) Ohm's constitutive law (2) written as $\mathbf{j}'^s = \boldsymbol{\sigma}'_s \mathbf{e}'^s$, where $\boldsymbol{\sigma}'_s$ is Ohm's constitutive matrix in $D'_s$. Thanks to (1b) written for steady-state fields, we have $\mathbf{e}'^s = -\mathbf{G}'_s \mathbf{v}'^s$, where $\mathbf{v}'^s$ is the array of electric scalar potentials associated with primal nodes in $D'_s$. We obtain the following algebraic equations in $D'_s$

$$\mathbf{G}'^T_s \boldsymbol{\sigma}'_s \mathbf{G}'_s \mathbf{v}'^s = 0, \tag{5}$$

where it can be proved that stiffness matrix $\mathbf{G}'^T_s \boldsymbol{\sigma}'_s \mathbf{G}'_s$ is symmetric even though $\boldsymbol{\sigma}'_s$ may not be. We solve (5) with boundary conditions imposed by assigning potential $U^l$ on the set of nodes lying on $S_a$ (like $n_a$) and 0 on the other set on $S_b$ (like $n_b$), $U^l$ being the voltage at coil leads. Thence, imposed voltages are $\mathbf{e}'^s = -\mathbf{G}'_s \mathbf{v}'^s$ for each edge of $D'_s$, and the array of currents, crossing dual faces of $D'_s$, is $\mathbf{j}'^s = \boldsymbol{\sigma}'_s \mathbf{e}'^s$.

### 3.1 Computation of $\mathbf{j}^s$ from $\mathbf{j}'^s$

Next, we need to compute $\mathbf{j}^s$ as in (4) with respect to $D_s$, from the knowledge of $\mathbf{j}'^s$ with respect to $D'_s$. We indicate with $S_a$ and $S_b$ the two faces of $S$, see Figure 2. The aim is to glue together pairs of broken dual volumes like $\tilde{n}_a$ and $\tilde{n}_b$ on the left and on the right of $S$ respectively, obtaining a dual volume $\tilde{n}$, where primal node $n \in S$. The boundary of a broken dual volume like $\tilde{n}_a$ is a collection of dual faces in $D'_s$ (like $\tilde{e}_1$ in Fig. 2) plus a face $f_a$ on $S_a$; similarly for $\tilde{n}_b$.

We indicate with $j_{n_a}$, $j_{n_b}$ the currents associated with faces $f_a$, $f_b$ respectively. From continuity law (1d), current $j_{n_a}$ can be expressed as the algebraic sum of currents crossing dual faces bounding $\tilde{n}_a$. Therefore current $j_{n_a}$ depends also on currents $j_a$ crossing dual faces like $\tilde{e}_a$, where the corresponding primal edge $e_a \in S$. Due to the structure of Ohm's matrix, such currents like $j_a$ are non null even though the voltage associated with edge $e_a$ is null. A similar reasoning applies to $j_{n_b}$ and $j_b$ currents.

Since the simplicial mesh on the left and on the right of $S$ is usually non symmetric with respect to $S$ and due to the structure of Ohm's matrix, then $j_{n_a} \neq j_{n_b}$ holds. This mismatch is local.

Now, to compute total currents, we may write $S_a = \bigcup_k f_{a_k}$, $S_b = \bigcup_k f_{b_k}$, where $f_{a_k}$, $f_{b_k}$ are the $k$-th $f_a$, $f_b$ surfaces. Then $J(S_a) = \sum_k j_{n_{a_k}}$, $J(S_b) = \sum_k j_{n_{b_k}}$ are the total currents crossing surfaces $S_a$ and $S_b$. They can be expressed as the algebraic sum of currents on a collection of dual faces (like $\tilde{e}_1$ in Fig. 2) on the left and on the right of $S$, where dual faces like $\tilde{e}_a$ give no contribution. Therefore, due to continuity law in $D'_c$, for total currents $J(S_a) = J(S_b)$ holds.

Next, to glue dual volumes like $\tilde{n}$ – nodes like $n$ are on the cutting plane $S$ – we need to glue the pairs of dual faces like $\tilde{e}_a$, $\tilde{e}_b$ (note that edges $e_a$, $e_b$ are on $S_a$, $S_b$ respectively). We obtain $\tilde{e}_a \bigcup \tilde{e}_b = \tilde{e}$, and for the corresponding currents $j_a + j_b = j$ holds. In this way we construct a new array of currents $\mathbf{j}^s$.

However, the local mismatch $j_{n_a} \neq j_{n_b}$ implies that continuity law (1d) is not satisfied locally, and this causes $(\mathbf{G}^T \mathbf{j}^s)_n \neq 0$, $\forall\, n \in S$.

### 3.2 A way to force consistency of $\mathbf{j}^s$

If $j_n = (\mathbf{G}^T_s \mathbf{j}^s)_n \neq 0$, we should compute $j_n$ explicitly to form the right hand side of the 4-th set of equations in (3). To avoid this, it is more efficient to set $j_n = 0$ and to modify $\mathbf{j}^s$ in (4) in order to comply with (1d), for each $\tilde{n} \in D_s$.

To this aim, we find a tree and the corresponding co-tree subgraphs in the graph formed by primal edges $e$ and nodes $n$ in $D_s$. We use currents $j^s$, associated with the co-tree edges, in order to recompute the currents associated with the edges of the tree to comply with (1d). To this purpose we considered the algorithm:

- For every node, find the star of edges around it.
- If all the edges of the cluster but one are marked with known current, then the current on the remaining free edge can be calculated from (1d).
- The edge is marked with known current and the node is removed from the list.

Then the algorithm proceeds cycling the list of nodes, until the list is empty. To set up the algorithm we consider

- as known and fixed the currents in the array $\mathbf{j}^s$ associated with dual faces crossed by a co-tree edge;
- a list of all nodes in $D_s$.

The algorithm converges in a few iterations and the computation time is negligible. This way we determine a new set of currents consistent with (1d).

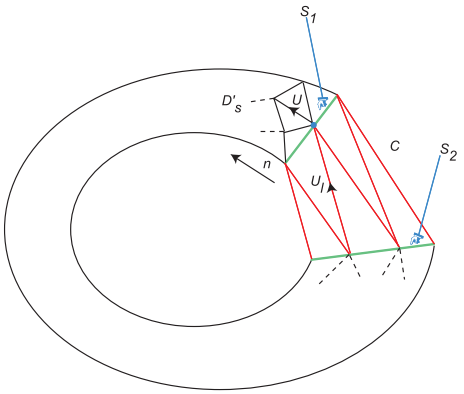


**Fig. 3.** Schematic view of the source region made of $D'_s$ and $C$ regions.

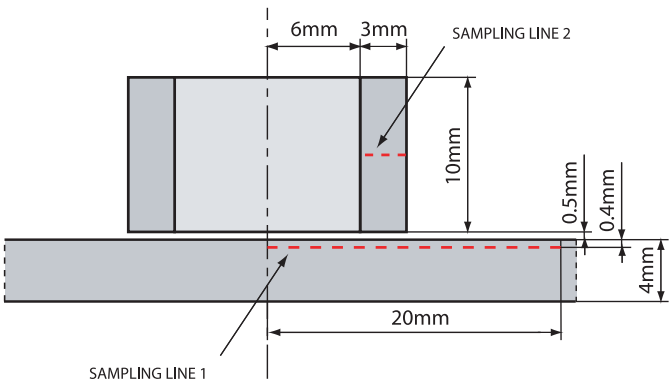


**Fig. 4.** Geometry of the test problem.

## 4 Localized voltage source

In the distributed Voltage Source Approach, we computed voltages associated with all the edges of $D'_s$ by means of the solution of the steady-state conduction problem (5). To avoid this step, we will describe here the Localized Voltage Source approach also referred to as "generalized source potential" in [7].

We redefine the cutting domain $C$ as made of one layer of tetrahedra, Figure 3, but now $C$ is assumed to be conductive with the same conductivity as $D_s$. Next, we indicate with $D'_s$ the complement of $C$ in $D_s$ and we introduce a source voltage distribution in $D_s$ having $C$ as support. We assume that the voltages along all the edges in $C$ have the same value $U_l$, while the imposed voltages on the edges of $D'_s$ are null.

We indicate with n the vector normal to the cross-section $S_1$ between $D'_s$ and $C$, pointing from $C$ to $D'_s$. Therefore, the array $\mathbf{u}_s$ becomes

$$\mathbf{u}_s = \mathbf{z}^T U_l, \tag{6}$$

where $U_l$ is the voltage at coil leads and array $\mathbf{z}$ is indexed over the edges of $D_s$; its $i$-th entry is $\pm 1$ if the edge is in $C$, otherwise it is zero. The entry is $+1$ if the inner orientation of the edge and the normal $n$ match.

In this way we concentrate the sources in the $C$ region, where the known voltage is specified on its edges without the need of solving a steady-state conduction current problem. With this approach it is not necessary to construct a special mesh in the region $C$ or to mesh a plane and then grow the transition layer on one side of it. We need only a thick cut in the coil. However we observe that the term $(\mathbf{G}^T \sigma \mathbf{u}^s)_n$ is not zero in the last equation of (3).

## 5 Numerical results

As reference 3D test problem, we considered a circular coil (10 mm of height, 12 mm of inner diameter, 18 mm of outer diameter) placed above an aluminium plate (4 mm of thickness), Figure 4. The coil is fed with a sinusoidal voltage at leads $U^l = 100$ V with a frequency $f = 5000$ Hz.

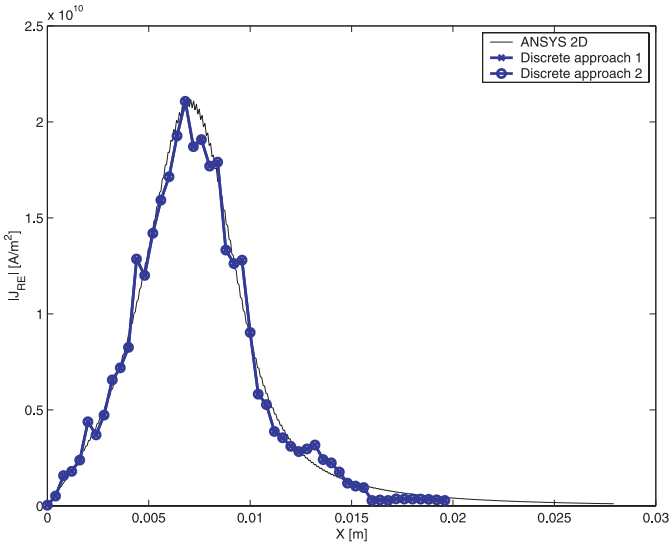


**Fig. 5.** The absolute values of the real parts of current density along $l_1$.

The primal mesh in $D$ consists of 82 369 tetrahedra the 29% of them is in the conducting regions.

We solved the test problem using the discrete geometric approach with the two proposed strategies for modeling the voltage source. For comparison, since the problem is axisymmetric, we also considered the results provided by a 2D Finite Elements analysis obtained using a commercial code. The absolute values of real and imaginary parts of the eddy-current density vector sampled along two lines $l_1$ and $l_2$ ($l_1$: length 20 mm, 0.4 mm below conductor's surface, $l_2$: length 3 mm, at half height of the coil, Fig. 4) are shown in Figures 5, 6, 7 and 8 respectively. The two approaches lead to practically coincident results, while the mismatch in the comparison along line $l_2$ with the reference values from finite elements is due to a poor discretization along the thickness of the coil and in addition we avoided any smoothing of the computed data. The CPU time needed to solve the linear systems iteratively on a portable PENTIUM IV 1.9 GHz, 512 MB of RAM are about 1.5 min for both the approaches (the distributed voltage source approach converges in 168 iterations while the localized voltage source approach in

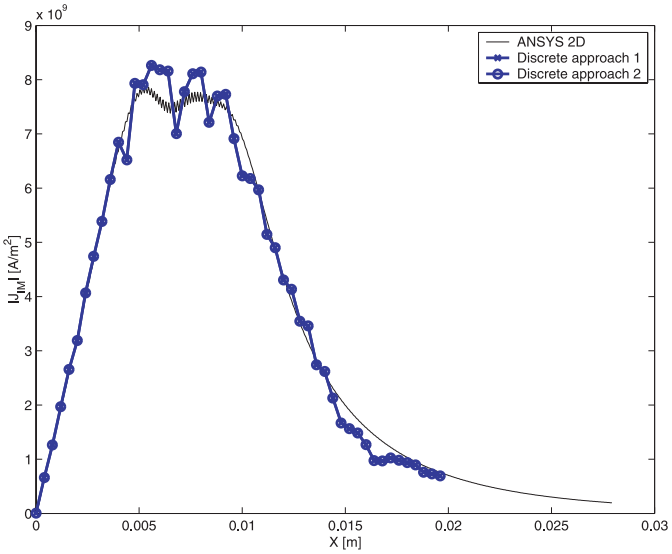


**Fig. 6.** The absolute values of the imaginary parts of current density along $l_1$.

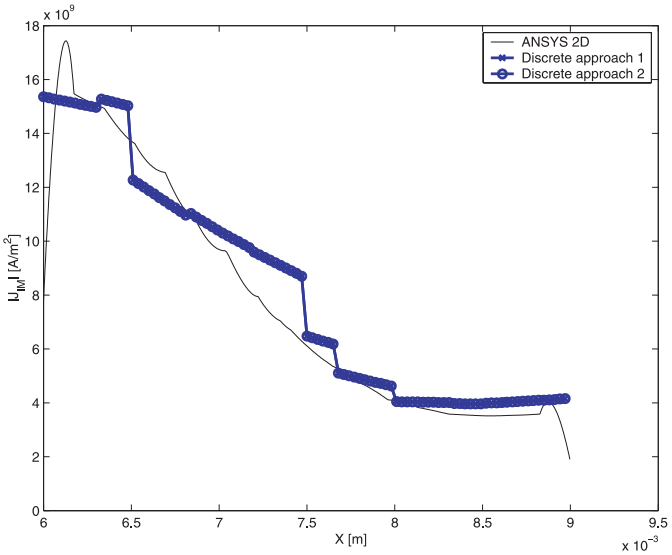


**Fig. 7.** The absolute values of the real parts of current density along $l_2$.

176 iterations, with relative residual of $10^{-5}$); the distributed voltage source approach needs 5 s of additional CPU time to solve the steady-state conduction current problem.

## 6 Conclusion

We have presented a pair of possible approaches to treat voltage driven coils of arbitrary shapes in eddy-current problems within a geometric $a-\chi$ formulation. An algorithm to make the right hand side of the final linear system consistent is also proposed. The methods have been tested against a reference 3D problem. The results obtained are in a good agreement to each others and with the results from a 2D Finite Element code.

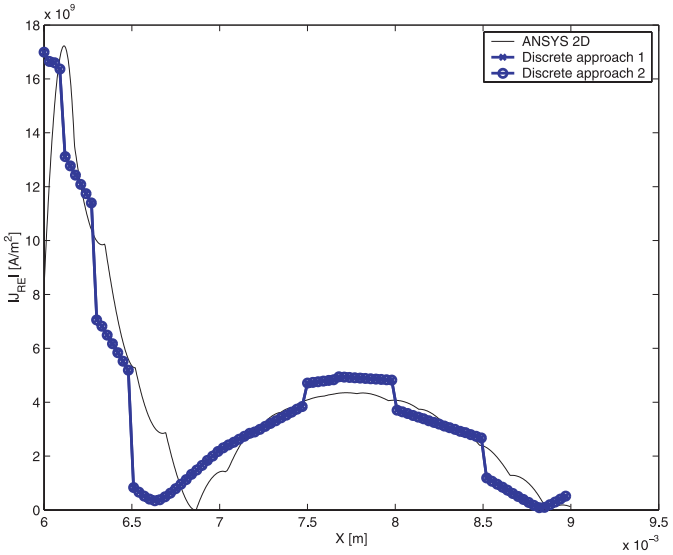


**Fig. 8.** The absolute values of the imaginary parts of current density along $l_2$.

## References

1. O. Biro, K. Preis, IEEE T. Magn. **25**, 4 (1989)
2. O. Biro, K. Preis, G. Buchgraber, I. Tičar, IEEE T. Magn. **40**, 1286 (2004)
3. A. Bossavit, IEEE T. Magn. **34**, 2429 (1998)
4. L. Codecasa, V. Minerva, M. Politi, IEEE T. Magn. **40**, 1414 (2004)
5. M. Cinalli, F. Edelvik, R. Schuhmann, T. Weiland, Int. J. Numer. Model. El. **17**, 487 (2004)
6. A. Bossavit, L. Kettunen, IEEE T. Magn. **36**, 861 (2000), DOI: 10.11/09/20.877580
7. P. Dular, F. Henrotte, W. Legros, IEEE T. Magn. **35**, 1630 (1999)
8. A. Kameari, K. Koganezawa, IEEE T. Magn. **33**, 1223 (1997)
9. H. Igarashi, T. Honma, IEEE T. Magn. **38**, 565 (2002)
10. F. Trevisan, IEEE T. Magn. **40**, 1314 (2004)
11. F. Trevisan, L. Kettunen, IEEE T. Magn. **40**, 361 (2004)
12. R. Specogna, F. Trevisan, IEEE T. Magn. **41**, 1259 (2005)
13. T. Tarhasaari, L. Kettunen, A. Bossavit, IEEE T. Magn. **55**, 1494 (1999)
14. E. Tonti, IEEE T. Magn. **38**, 333 (2002)
15. E. Tonti, Algebraic topology and computational electromagnetism, *4th International Workshop on Electric and Magnetic Fields, Marseille, France, 12–15 May 1988*, pp. 284–294
16. B. Weiss, O. Biro, IEEE T. Magn. **40**, 957 (2004)
17. S. Reitzinger, M. Kaltenbacher, IEEE T. Magn. **38**, 477 (2002)